2014

Evaluation of ANN Estimation-Based MPPT Control for a DFIG Wind Turbine

Chun Wei
University of Nebraska-Lincoln, cwei@huskers.unl.edu

Liyan Qu
University of Nebraska-Lincoln, lqu2@unl.edu

Wei Qiao
University of Nebraska–Lincoln, wqiao@engr.unl.edu

Power Electronics and Machines for Wind and Water Applications (PEMWA), 2014 IEEE Symposium
Pages: 1 - 6, DOI: 10.1109/PEMWA.2014.6912224

Evaluation of ANN Estimation-Based MPPT Control for a DFIG Wind Turbine

Chun Wei, Liyan Qu, and Wei Qiao
Power and Energy Systems Laboratory
Department of Electrical Engineering
University of Nebraska−Lincoln
Lincoln, NE 68588-0511 USA
cwei@huskers.unl.edu; lqu2@unl.edu; wqiao@engr.unl.edu

Abstract—**This paper proposes an artificial neuronal network (ANN) estimation-based wind speed sensolress MPPT algorithm for wind turbines equipped with doubly-fed induction generators (DFIG). The ANN is designed to produce the optimal control signal for the DFIG power or speed controller. The optimal parameters of the ANN are determined by using a particle swarm optimization (PSO) algorithm. A 3.6 MW DFIG wind turbine is simulated in PSCAD to evaluate and compare the proposed MPPT method with the traditional tip speed ratio (TSR) and turbine power profile-based MPPT methods in both the speed control and power control modes in variable wind speed conditions.**

I. INTRODUCTION

Wind power has been extensively developed in the last decade and might be a major alternative for electricity supply in the near future because of its plenitude, renewability, and wide distribution [1]. Among different wind turbine technologies, the DFIG wind turbines dominate the total installed wind turbine capacity. When the wind speed is between the cut-in and rated values, the rotor speed of a DFIG can be optimally adjusted to achieve the maximum wind power extraction [2].

Different MPPT control methods have been proposed for DFIG wind turbines and they mainly fall into two categories: wind speed measurement-based methods, in which the information of wind speed is obtained from sensors, such as anemometers, and sensorless methods without using wind speed measurements [3]. The TSR control and turbine power profile-based control are two commonly used wind speed measurement-based MPPT methods. In the TSR control, the rotor speed control signal is modified to follow the measured variable wind speed to maintain the TSR at its optimal value for maximum wind power extraction [4]. In the turbine power profile-based control, when the wind speed signal is obtained, the optimal power control signal will be generated from the curve of optimal output power versus wind speed, which is usually provided by the wind turbine manufacturer, for MPPT control of the wind turbine. Although these two methods are easy to implement, their performance largely depends on the wind speed information provided by the anemometer, which may not be accurate. In addition, the total installation cost of the wind turbine system increases due to the use of mechanical sensors.

To solve the problems of using wind speed sensors, mechanical sensorless MPPT control methods have been developed. These include the power signal feedback control, optimal torque control, hill climbing control, and fuzzy logic control. These methods are based on either the wind turbine characteristics or a perturb and observe (P&O) method [3], [5], [6]. References [7]-[9] proposed methods of using an ANN to estimate the wind speed information for sensorless MPPT control of wind turbines. In these methods, wind speed is estimated from the mechanical power and rotor speed of the wind turbine to calculate the optimum rotor speed control signal. Since many MPPT methods have been reported in the literature, it is valuable to evaluate and compare different MPPT methods to determine one that is most suitable for a wind turbine.

This paper compares the ANN estimation-based MPPT method with the traditional TSR and turbine power profile-based methods from the perspective of system dynamic speed and power responses in variable wind speed conditions for a 3.6 MW DFIG wind turbine. Both the speed control and power control modes are considered for the DFIG. The rest of the paper is organized as follows. Section II gives an introduction of the DFIG wind turbine and its control modes; Section III presents the ANN estimation-based MPPT methods for both the speed control mode and power control mode; simulation results are provided and discussed in Section IV; and conclusions are drawn in Section V.

This work was supported in part by the U.S. National Science Foundation under grant ECCS-0901218 and CAREER Award ECCS-0954938.

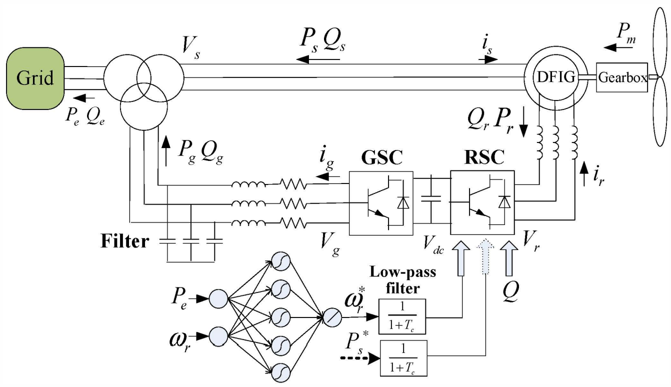

Fig. 1. A DFIG wind turbine with the ANN estimation-based MPPT control.

II. DFIG-Based Wind Energy Conversion System

A. System Configuration

Fig. 1 shows the block diagram of a DFIG wind turbine equipped with the proposed ANN estimation-based MPPT control. The stator of the DFIG is connected directly to a power grid while the rotor is fed to the power grid through a back-to-back power electronic converter system to achieve variable-speed operation and constant-frequency control. The stator flux-oriented or stator voltage-oriented vector control method is utilized to control the rotor side converter (RSC) to achieve decoupled control of different quantities (e.g., speed, power or torque, and stator voltage or reactive power) of the DFIG. The control objective of the grid side converter (GSC) is to maintain a constant dc-link voltage and a unity power factor during normal operation, and to provide reactive power during a grid fault if possible [10]. The back-to-back converter system enables the induction generator to operate in the subsynchronous and supersynchronous modes, which enables the wind turbine to capture more wind energy when the wind speed changes.

B. Control Modes of the DFIG

In this paper, the speed control mode and power control mode are chosen for comparison of the ANN estimation-based MPPT method with the traditional TSR and turbine power profile-based MPPT methods.

1) Speed control mode: In the speed control mode, the reference of i_{qr} is obtained from the output of a PI rotor speed controller as shown in Fig. 2, in which i_{dr}, i_{qr} and u_{qr} are the d-axis and q-axis rotor currents and the uncompensated q-axis rotor voltage, respectively; U_s is the magnitude of the grid voltage; ψ_s is the magnitude of the stator flux; ω_s, ω_r and ω_{slip} are the synchronous speed, rotor speed and slip frequency, respectively; L_s, L_r and L_m are the self-inductance of the stator and rotor and their mutual inductance, respectively; T_m and T_e are the mechanical and electrical torque, respectively; J is the moment of inertia; p is the number of pole pairs; r_r is the rotor resistance and $\sigma = 1 - L_m^2/(L_s L_r)$.

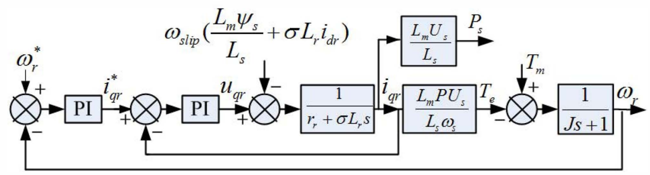

Fig. 2. Block diagram of the speed control mode.

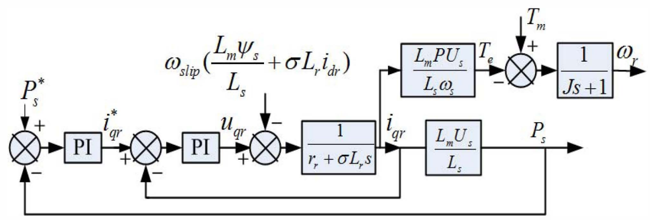

Fig. 3. Block diagram of the power control mode.

2) Power control mode: In the power control mode, the reference of i_{qr} is obtained from the output of a PI power controller, whose input is the difference between the reference and actual stator active powers, as illustrated by Fig. 3.

III. ANN Estimation-Based MPPT

A. The Principle of ANN Estimation-Based MPPT Method

The total power P_m that a wind turbine is able to capture from wind can be calculated by the following formula.

$$P_m = \frac{1}{2}\rho A v_w^3 C_p(\lambda, \beta) \tag{1}$$

where ρ is the air density, $A = \pi R^2$ is the area swept by the blades and R is the blade radius, v_w is the wind speed, and C_p is the power coefficient, which is determined by the TSR $\lambda = \omega_t R / v_w$ and the blade pitch angle β, where ω_t is the turbine rotating speed.

Fig. 4 shows the turbine mechanical power versus rotor speed characteristics of the wind turbine used in this paper for different wind speeds. For each wind speed, there is only one optimum rotor speed at which the maximum wind power is extracted. In addition, there is only one power-speed curve for a specific wind speed. As a result, the wind speed v_w can

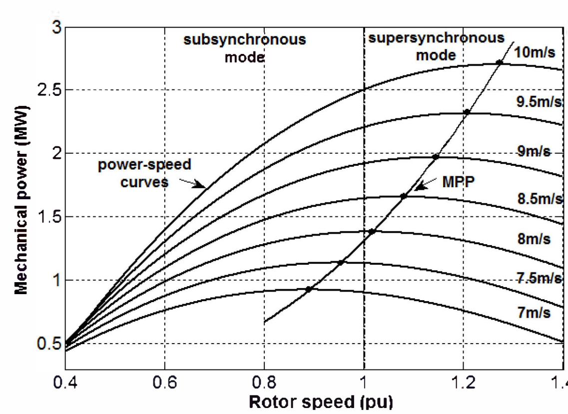

Fig. 4. Mechanical power vs. rotor speed characteristics of the wind turbine.

be estimated if the mechanical power P_m and rotor speed ω_r are known. Once the wind speed information is obtained, the optimal rotor speed control signal ω_r^* or the optimal stator power control signal P_s^* can be derived from the power-speed characteristic curves.

B. Speed Control Mode

The optimal rotor speed control signal ω_r^* can easily be calculated when the wind speed is estimated. However, the acquisition of the turbine mechanical power is relatively difficult in practical applications because only the electrical power of the generator will be measured. A method to estimating the wind turbine mechanical power from the electrical power while taking into account the power losses can be found in [7]. If neglecting the power losses, the turbine mechanical power can be assumed to be the same as the generator electrical power in steady-state operating conditions.

C. Power Control Mode

Even the mechanical power is known, it cannot be set as the stator power control signal directly because the total output power of a DFIG is the sum of the stator power P_s and the rotor power P_r, as indicated in Fig. 1. Neglecting the power losses and assuming the DIFG is reactive neutral, the stator and rotor power can be calculated by following two formulas [11]:

$$P_s = \frac{1}{1-s} P_m \tag{2}$$

$$P_r = \frac{s}{1-s} P_m \tag{3}$$

where s is the slip. Once the wind speed is estimated, the optimum rotor speed and the corresponding slip can be calculated; then the optimum stator power control signal can be obtained from (2). Reference [12] presents an approach to determine the optimum stator power when the power losses are taken into account.

D. PSO-Trained ANN-Based Optimal Control Signal Estimation

1) ANN-based estimation: A three-layer, feedforward ANN with five neurons and the sigmoid activation function in the hidden layer is designed to establish the mapping from the electrical power and rotor speed to the optimum rotor speed ω_r^* or optimum stator power P_s^*, as shown in Fig. 5.

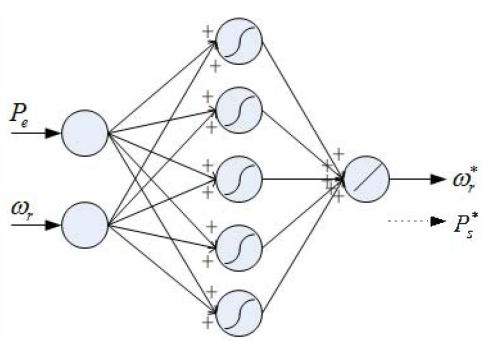

Fig. 5. Optimal control signal estimation using a three-layer, feedforward ANN.

The output of the ANN is

$$\omega_r^* \text{ or } P_s^* = \sum_{i=1}^{5} \frac{v_i}{1+e^{-(w_{i1}P_e + w_{i2}\omega_r)}} \tag{4}$$

where w_{ij} are the weights between the input and hidden layers, and v_i are the weights between the hidden and output layers. The ANN is trained such that the weights are updated to minimize the mean square error between the ANN output (ω_r^* or P_s^*) and its actual value for all the training data samples.

2) ANN training using PSO: In this paper, the PSO algorithm [13] is used to train the weights of the ANN. First, a population of particles with random positions and velocities is initialized, where all the elements of each particle's position and velocity vectors are within [-1, 1]. The position vector of each particle contains 15 elements, which are the weights of the ANN to be trained as follows,

$$x_i = [w_{11}, w_{21}, w_{31}, w_{41}, w_{51}, w_{12}, w_{22}, w_{32}, w_{42}, w_{52}, v_1, v_2, v_3, v_4, v_5] \tag{5}$$

where x_i is the position vector of the ith particle, $i = 1, \cdots, N$ and N is the total number of particles. The fitness function is the mean square error between the ANN-estimated control signal and the actual optimum control signal for all the training data samples. The velocity and position of each particle are updated according to the following two equations:

$$\vec{v}(t) = w\vec{v}(t-1) + c_1 r_2 \left(\overrightarrow{pbest} - \vec{x}(t-1)\right) + c_2 r_2 \left(\overrightarrow{gbest} - \vec{x}(t-1)\right) \tag{6}$$

$$\vec{x}(t) = \vec{x}(t-1) + \vec{v}(t) \tag{7}$$

where t is the current iteration number of the PSO implementation; *pbest* is the best position of the particle leading to the smallest fitness up to the current iteration t; *gbest* is the best position of all particles leading to the minimum fitness value of all particles up to the current iteration t; w is the inertia weight; c_1 and c_2 are acceleration coefficients; r_1 and r_2 are two uniformly distributed random numbers between 0 and 1. The performance of the PSO algorithm highly depends on the neighborhood topology and the following parameters: the size of the population N, acceleration coefficients, maximum velocity $v_{\max}$, and inertia weight [14]. Table 1 lists the parameters of the PSO used for training the ANN weights in this paper.

The optimum control signals produced by the PSO-trained ANN are used to control the DFIG in different control modes, as illustrated in Fig. 1. A low-pass filter is added in between to smooth the output of the ANN.

IV. Simulation Results and Discussions

Simulation studies are carried out in PSCAD for a 3.6-MW DFIG wind turbine [7]. The training data for the ANN

Table I. PSO parameters applied for ANN training.

Topology	N	Iteration number	w	c_1	c_2	$v_{\max}$
Gbest	30	1000	0.75	1.9	1.9	10

are obtained by simulating the DFIG wind turbine for different operating conditions. During the simulation, the wind speed and rotor speed signals are set with an increments of Δv_w = 0.1 m/s and $\Delta\omega_r$ = 0.05 rad/s, respectively. The total electrical power P_e of the DFIG is measured for each point of the wind speed and rotor speed. The optimum rotor speed for each wind speed point is calculated and then is set to control the DFIG in the simulation to obtain the optimum stator power control signal. From the above process, the total electrical power and rotor speed can be used to directly obtain the optimum rotor speed ω_r^* for the speed control mode and the optimum stator power P_s^* for the power control mode. Such relationships are learned by the ANN using the training data obtained from the PSCAD simulation. The trained ANN is then used online to determine the optimum rotor speed or stator power control signal from the measured total electrical power and rotor speed for MPPT control of the wind turbine. Some typical simulation results are demonstrated and discussed below.

A. Control Signal Estimation Results

To verify the effectiveness of the ANN, the optimum control signals estimated from the ANN are compared with the actual optimum control signals under randomly variable wind speed conditions.

1) Power control signal estimation: Fig. 6 compares the ANN-estimated optimum stator power control signal with its actual values. It shows that the output of the ANN tracks the actual optimum control signal well with a maximum tracking error around 0.02 MW, which is only approximately 0.6% of the power rating of the DFIG.

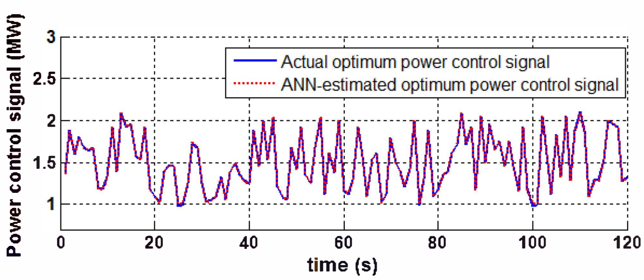

(a)

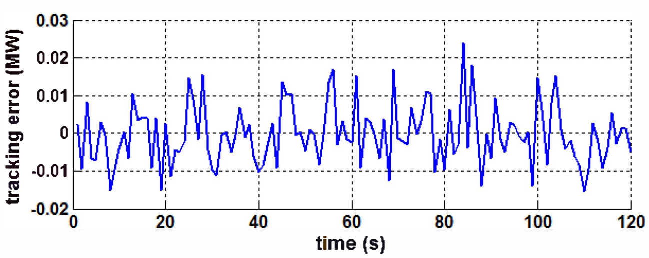

(b)

Fig. 6. Stator power control signal estimation. (a) Comparison of estimated and actual optimum control signals and (b) estimation error.

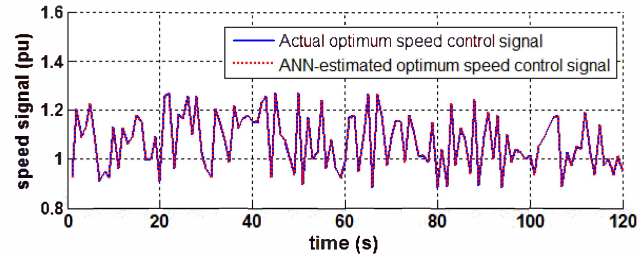

(a)

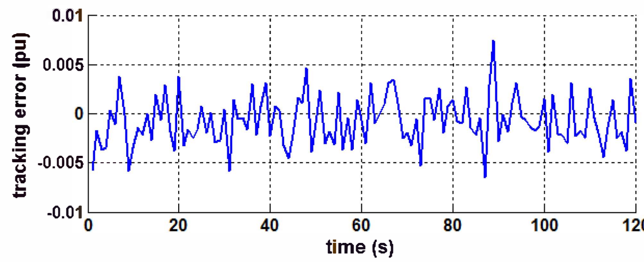

(b)

Fig. 7. Rotor speed control signal estimation. (a) Comparison of estimated and actual optimum control signals and (b) estimation error.

2) Speed control signal estimation: The estimation result of the optimum rotor speed control signal is displayed in Fig. 7. The maximum tracking error is about 0.5% of the rated rotor speed.

B. Comparison of MPPT Methods in Speed Control Mode

To compare the rotor speed and power responses of the ANN estimation-based MPPT method and the TSR-based MPPT method for variable wind speed conditions, a step change is applied to the wind speed during the simulation (Fig. 8). Except for different MPPT methods, all of the other parameters of the DFIG control system are identical in the same control mode.

In the speed control mode, the rotor speed has a faster response when using the TSR-based MPPT control (Fig. 9). This difference is mainly caused by different changing rates of the optimal speed control signals obtained from the two different methods when the wind speed varies. The optimal speed control signal changes quickly in response to the wind speed changes when using the TSR-based method (Fig. 10). As a consequence, the speed response is mainly influenced by the response time of the speed controller. However, in the ANN estimation-based method, the ANN uses the rotor speed and output power of the DFIG as its input. The rotor speed cannot change suddenly because of the system inertia, which leads to a gradual change in output of the ANN, from which the optimal speed control signal is obtained. Although the TSR-based method has a relatively faster response, one disadvantage can be seen from Fig. 11, where large power transients are observed during wind speed variations because of the large system inertia and the sudden changes of the speed control signal. However, the output power varies smoothly when using the ANN estimation-based method owing to the smooth transition of the rotor speed control signal.

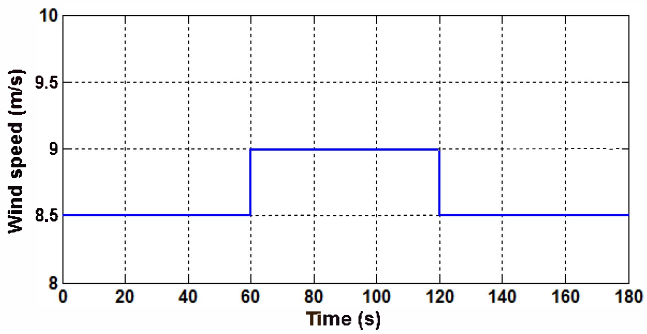

Fig. 8. Wind speed variations during the simulation

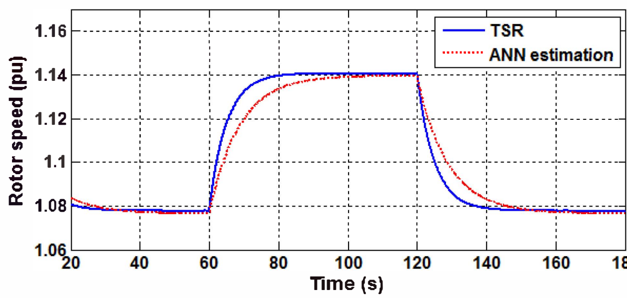

Fig. 9. Comparison of rotor speed responses in the speed control mode.

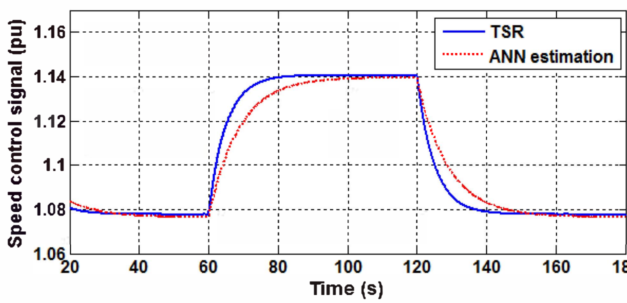

Fig. 10. Comparison of optimal speed control signals.

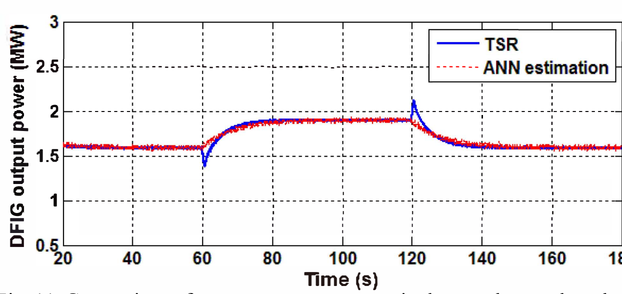

Fig. 11. Comparison of output power responses in the speed control mode.

C. *Comparison of MPPT Methods in Power Control Mode*

In the power control mode, the rotor speed responds much faster when using the ANN estimation-based MPPT control. As shown in Fig. 12, the rotor speed of the DFIG using the ANN estimation-based MPPT settles down to the steady state within about 20 s during wind speed variations, which is much shorter than that the case when using the turbine power profile-based MPPT. This difference is relevant to the control principles of the two methods. In the turbine power profile-based MPPT control, the optimum power control signal is changed quickly when the wind speed changes (Fig. 13). However, the current control loop (Fig. 3) is usually designed to have a fast response [10]. Therefore, the output stator power will match the reference power quickly. Once i_{qr} is fixed, the large difference between the electrical torque T_e and the mechanical torque T_m will mainly be reduced by the system damping, which causes a long speed response time. On the contrary, the optimum power control signal changes smoothly during wind speed variations when using the ANN estimation-based MPPT control. During this process, the rotor speed signal is used as a feedback to generate the optimal stator power control signal, thus decreasing the speed response time compared with the other method. Fig. 14 shows the comparison of output power responses in the power control mode. It shows that the ANN estimation-based MPPT control leads to a slower power response.

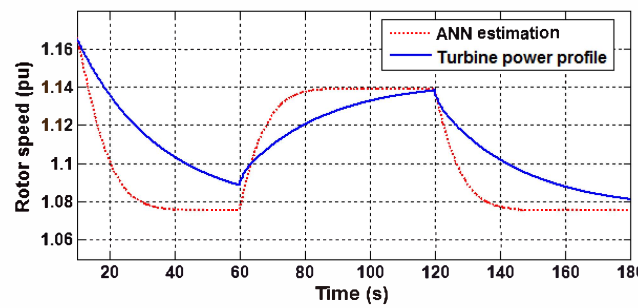

Fig. 12. Comparison of rotor speed responses in the power control mode.

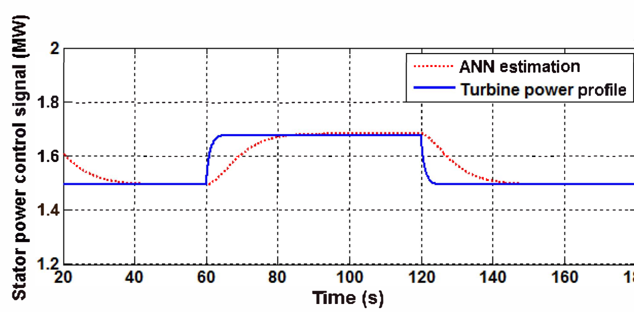

Fig. 13. Comparison of optimal power control signals

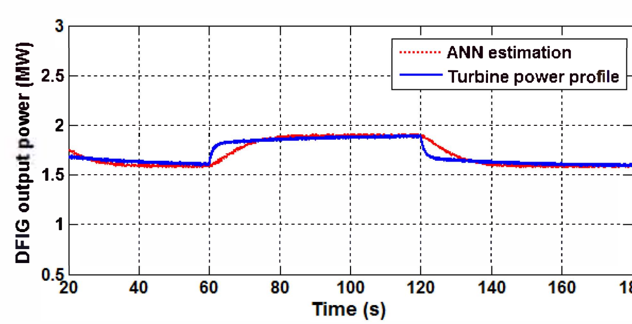

Fig. 14. Comparison of output power responses in the power control mode.

V. Conclusion

This paper has presented an ANN estimation-based MPPT algorithm for a MW-scale DFIG wind turbine operating in both speed and power control modes. The responses of the rotor speed and output power of the DFIG using the ANN estimation-based method have been compared with those of using the traditional TSR and turbine power profile-based methods during wind speed variations. Simulation studies have been performed in PSCAD for a 3.6 MW DFIG wind turbine equipped with the three MPPT control methods. Simulation results have shown that compared with the turbine power profile method, the ANN estimation-based method could decrease the speed response time and make the system settle down to the steady state faster in the power control mode and provide a smoother power transition than the TSR method in the speed control mode during wind speed variations. Therefore, the proposed ANN estimation-based MPPT control represents a better tradeoff in terms of the system dynamic speed and power responses.

References

[1] T. Jamasb, W. J. Nuttall, and M. G. Pollitt, *Future Electricity Technologies and System*. Cambridge: Cambridge University Press, 2006.

[2] B. Wu, Y. Q. Lang, N. Zargari, and S. Kouro, *Power Conversion and Control of Wind Energy Systems*. Hoboken, NJ: John Wiley & Sons, 2011.

[3] Y. Zhao, C. Wei, Z. Zhang, and W. Qiao, "A review on position/speed sensorless control for permanent magnet synchronous machine-based wind energy conversion systems," *IEEE Journal of Emerging and Selected Topics in Power Electronics*, vol. 1, no. 4, pp. 203-216, Dec. 2013.

[4] H. M. Kojabadi, L. C. Chang, and T. Boutot, "Development of a novel wind turbine simulator for wind energy conversion system using an inverter-controlled induction motor," *IEEE Trans. Energy Convers.*, vol. 19, no. 3, pp. 547-552, Sep. 2004.

[5] Q. Wang and L. C. Chang, "An intelligent maximum power extraction algorithm for inverter-based variable speed wind turbine systems," *IEEE Trans. Power Electron.*, vol. 19, no. 5, pp. 1242- 1249, Sept. 2004.

[6] M. G. Simoes, B. K. Bose, and R. J. Spiegel, "Fuzzy logic based intelligent control of a variable speed cage machine wind generation system," *IEEE Trans. Power Electron.*, vol. 12, no. 1, pp. 87-95, Jan. 1997.

[7] W. Qiao, W. Zhou, J. M. Aller, and R. G. Harley, "Wind Speed Estimation Based Sensorless Output Maximization Control for a Wind Turbine Driving a DFIG," *IEEE Trans. Power Electron.*, vol. 23, no. 3, pp. 1156-1169, May 2008.

[8] H. Li, K. L. Shi, and P. G. McLaren, "Neural-network-based sensorless maximum wind energy capture with compensated power coefficient," *IEEE Trans. Ind. Appl.*, vol. 41, no. 6, pp. 1548-1556, Nov/Dec 2005.

[9] W. Qiao, X. Yang, and X. Gong, "Wind speed and rotor position sensorless control for direct-drive PMG wind turbines," *IEEE Trans. Ind. Appl.*, vol. 48, no. 1, pp. 3-11, Jan/Feb 2012.

[10] R. Pena, J. C. Clare, and G. M. Asher, "Doubly fed induction generator using back-to-back PWM converters and its application to variable-speed wind-energy generation," *IEE Proc. Electric Power Appl.*, vol. 143, no. 3, pp. 231-241, May 1996.

[11] S. Muller, M. Deicke, and R. W. De Doncker, "Doubly fed induction generator systems for wind turbines," *IEEE Ind. Appl. Magazine*, vol. 8, no. 3, pp. 26-33, May/Jun 2002.

[12] W. Qiao, X. Gong, and L. Qu, "Output maximization control for DFIG wind turbines without using wind and shaft speed measurements," in *Proc. IEEE Energy Convers. Congr. Exposit.*, Sep. 2009, pp. 404-410.

[13] W. Qiao and R.G. Harley, "Optimization of radial basis function widths using particle swarm optimization," in *Proc. IEEE Swarm Intelligence Symposium*, May 2006, pp. 55-60.

[14] R. Eberhart and J. Kennedy, "A new optimizer using particle swarm theory," in *Proc. 6th Int. Symp. Micro Machine and Human Science*, Oct. 1995, pp.39-43.